J|A|C|S
ARTICLES
Published on Web 03/20/2004

The Optical and Charge Transport Properties of Discotic Materials with Large Aromatic Hydrocarbon Cores

Michael G. Debije,[†] Jorge Piris,[†] Matthijs P. de Haas,[†] John M. Warman,*[,†] Željko Tomović,[‡] Christopher D. Simpson,[‡] Mark D. Watson,[‡] and Klaus Müllen[‡]

Contribution from the Radiation Chemistry Department, IRI, Delft University of Technology, Mekelweg 15, 2629 JB Delft, The Netherlands, and Max-Planck-Institut für Polymerforschung, Ackermannweg 10, D-55128 Mainz, Germany

Received November 14, 2003; E-mail: warman@iri.tudelft.nl

Abstract: The optical absorption and charge transport properties of a series of discotic molecules consisting of peripherally alkyl-substituted polycyclic aromatic cores have been investigated for core sizes, n, of 24, 42, 60, 78, 96, and 132 carbon atoms. In dilute solution, the wavelength maximum of the first absorption band increases linearly with n according to $\lambda_{max} = 280 + 2n$ and the spectral features become increasingly broadened. The two smallest core compounds display a slight red-shift and increased spectral broadening in spin-coated films. For derivatives with $n = 24$, 42, 60, and 96, the one-dimensional, intracolumnar charge mobility, $\Sigma\mu_{1D}$, was determined using the pulse-radiolysis time-resolved microwave conductivity technique. For the compounds which were crystalline solids at room temperature, $\Sigma\mu_{1D}$ lay within the range 0.4−1.0 cm^2/Vs. In the discotic mesophases at ca. 100 °C, $\Sigma\mu_{1D}$ was somewhat lower and varied from 0.08 to 0.38 cm^2/Vs. The mobility values in both phases are considerably larger than the maximum values found previously for discotic triphenylene derivatives. However, the recently proposed trend toward increasing mobility with increasing core size is not substantiated by the results on the present series of increasingly large aromatic core compounds.

Introduction

Discotic liquid crystalline materials have been proposed for some time as potential candidates for the active layer in organic-based optoelectronic devices such as light-emitting diodes (LEDs), photovoltaic cells (PVCs), and field-effect transistors (FETs). Recently, working PVC and FET devices based on peripherally substituted hexabenzocoronene derivatives have been demonstrated.[1,2] The particular suitability of discotics for these applications relies on their ability to self-assemble into columnar stacks which facilitate the one-dimensional transport of charge.[3−12] Trap-free mobilities have been determined for discotic materials which are at least as large as those found for conjugated polymers and approach values on the order of 1 cm^2/Vs, similar to those found for single-crystal organic materials.[13] The suitability of discotics for practical applications has been enhanced by the recent discovery that highly aligned films can be readily solution-processed by self-assembly on a friction-deposited poly-tetrafluoroethylene primer layer,[2,14−16] or by zone-casting onto an untreated glass substrate.[17]

In addition to their potential function as charge transport layers, discotic materials display a diversity of optical properties which could be important in PVC and LED applications. Their absorptive and emissive properties can be tailored to suit a particular application by modification of the central (hetero)-aromatic core.[18] We have also recently found that the optical dichroism of aligned layers formed by zone-casting can be

[†] Delft University of Technology.
[‡] Max-Planck-Institut für Polymerforschung.

(1) Schmidt-Mende, L.; Fechtenkötter, A.; Müllen, K.; Moons, E.; Friend, R. H.; MacKenzie, J. D. *Science* **2001**, *293*, 1119−1122.
(2) van de Craats, A. M.; Stutzmann, N.; Bunk, O.; Nielsen, M. M.; Watson, M.; Müllen, K.; Chanzy, H. D.; Sirringhaus, H.; Friend, R. H. *Adv. Mater.* **2003**, *15*, 495−499.
(3) Schouten, P. G.; Warman, J. M.; de Haas, M. P.; van Nostrum, C. F.; Gelinck, G. H.; Nolte, R. J. M.; Copyn, M. J.; Zwikker, J. W.; Engel, M. K.; Hanack, M.; Chang, Y. H.; Ford, W. T. *J. Am. Chem. Soc.* **1994**, *116*, 6880−6894.
(4) Schouten, P. G.; Warman, J. M.; de Haas, M. P.; Fox, M.-A.; Pan, H.-L. *Nature* **1991**, *353*, 736−737.
(5) Adam, D.; Haarer, D.; Closs, F.; Frey, T.; Funhoff, D.; Siemensmeyer, K.; Schuhmacher, P.; Ringsdorf, H. *Ber. Bunsen-Ges. Phys. Chem.* **1993**, *97*, 1366−1370.
(6) van de Craats, A. M.; Warman, J. M.; de Haas, M. P.; Adam, D.; Simmerer, J.; Haarer, D.; Schuhmacher, P. *Adv. Mater.* **1996**, *8*, 823−826.
(7) Adam, D.; Schuhmacher, P.; Simmerer, J.; Häussling, L.; Siemensmeyer, K.; Etzbach, K. H.; Ringsdorf, H.; Haarer, D. *Nature* **1994**, *371*, 141−143.
(8) Boden, N.; Bushby, R. J.; Cammidge, A. N.; Clements, J.; Luo, R.; Donovan, K. J. *Mol. Cryst. Liq. Cryst.* **1995**, *261*, 251−257.
(9) Kreouzis, T.; Donovan, K. J.; Boden, N.; Bushby, R. J.; Lozman, O. R.; Liu, Q. *J. Chem. Phys.* **2001**, *114*, 1797−1802.
(10) Ochse, A.; Kettner, A.; Kopitzke, J.; Wendorff, J. H.; Bässler, H. *Phys. Chem. Chem. Phys.* **1999**, *1*, 1757−1760.
(11) van de Craats, A. M.; Warman, J. M.; Fechtenkötter, A.; Brand, J. D.; Harbison, M. A.; Müllen, K. *Adv. Mater.* **1999**, *11*, 1469−1472.
(12) Warman, J. M.; van de Craats, A. M. *Mol. Cryst. Liq. Cryst.* **2003**, *396*, 41−72.
(13) Karl N.; Kraft, K.-H.; Marktanner, J.; Münch, M.; Schatz, F.; Stehle, R.; Uhde, H.-M. *J. Vac. Sci. Technol.* **1999**, *A17*, 2318−2328.
(14) Zimmermann, S.; Wendorff, J. H.; Weder, C. *Chem. Mater.* **2002**, *14*, 2218−2223.
(15) Piris, J.; Debije, M. G.; Stutzmann, N.; van de Craats, A. M.; Watson, M.; Müllen, K.; Warman, J. M. *Adv. Mater.* **2003**, *15*, 1736−1740.
(16) Bunk, O.; Nielsen, M. M.; Sølling, T. I.; van de Craats, A. M.; Stutzmann, N. *J. Am. Chem. Soc.* **2003**, *125*, 2252−2258.
(17) Tracz, A.; Jeszka, J. K.; Watson, M. D.; Pisula, W.; Müllen, K.; Pakula, T. *J. Am. Chem. Soc.* **2003**, *125*, 1682−1683.
(18) Watson, M. D.; Fechtenkötter, A.; Müllen, K. *Chem. Rev.* **2001**, *101*, 1267−1300.

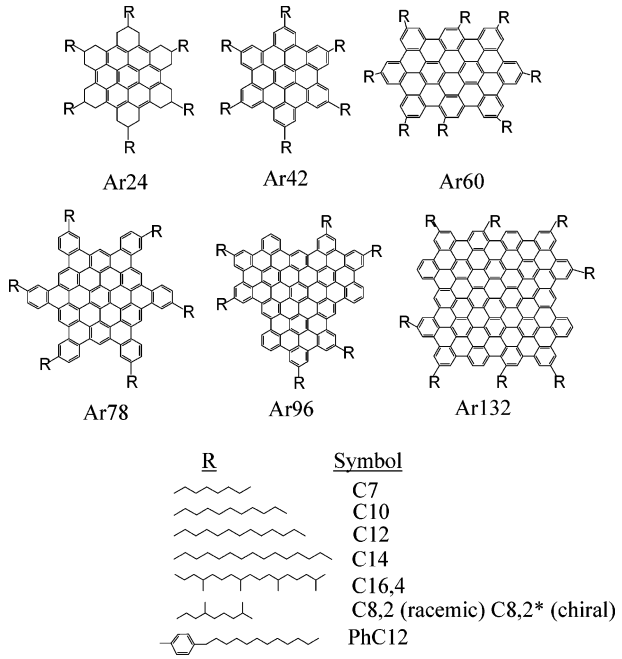

Figure 1. The molecular structures of the compounds investigated. The molecules are designated in the text by the following notation: "Ar*n*(*R*)*m*" with *n* the number of aromatic carbon atoms in the core, *R* the symbol for the type of peripheral chains (as given in the figure), and *m* their number.

switched on or off depending on whether the planes of the aromatic cores are oriented perpendicular or are tilted with respect to the columnar axis.[19] This opens up the possibility of additional applications in the areas of optical switching and data storage devices.

In this work, we present measurements of the optical absorption and charge transport properties of a series of discotic materials based on molecules with aromatic hydrocarbon cores consisting of 24, 42, 60, 78, 96, and 132 carbon atoms. One aim of this study was to investigate the general validity of the recent prediction that the mobility of charge should increase with increasing size of the core.[20]

Experimental Section

The molecular structures of the compounds investigated are shown in Figure 1.

The pseudonyms used in the text are based on the notation "Ar*n*(*R*)-*m*" with *n* the number of carbon atoms in the aromatic core, and *R* and *m* the nature and number of the peripheral substituents, as indicated in Figure 1. References to the methods of synthesis, purification, and characterization of specific compounds are given in the third column of Table 1. Many of the compounds display a strong tendency to aggregate and are only weakly soluble in common organic solvents. Because of this, rigorous purification of the Ar78 and Ar132 derivatives was not possible.

Optical absorption spectra of dilute solutions in chloroform were recorded using a Perkin-Elmer Lambda 40 UV/Vis spectrophotometer. Spectra of ca. 150-nm-thick films, prepared by spin-coating chloroform solutions onto quartz substrates, were recorded using a Perkin-Elmer Lambda 900 spectrophotometer equipped with an integrating sphere. In the latter case, the optical density, OD, was determined from $OD = -\log_{10}[F_T/(1 - F_R)]$ with F_T and F_R the fraction of light transmitted and reflected by the sample, respectively.

Table 1. Wavelength Maxima of the First Absorption Band and One-Dimensional Mobility Values Determined from the End-of-Pulse Conductivity[e]

					$\Sigma\mu_{1D}$ [10^{-2} cm^2 V^{-1}s^{-1}]			
core	mantle	refs	λ_{max} (nm)	T^d (K→D) (°C)	RT	T (K→D) −10 °C	T (K→D) +10 °C	D phase (calcd)[c]
Ar24	(C12)6	23	331	ca. 100	72	76	10−20	9
Ar42	(C14)6	27		109	100	113	31	42
	(C12)6	27−3 0		105	70	96	38	
	(C8,2*)6	31		99	46	54	26	
	(C8,2)6	31	361	81	43	62	30	
	(C10)6	27		124	40	55	26	
	(PhC12)6	29, 3 0		[a]	22		31[b]	
Ar60	(C12)8	32	410	102	52	80	26	75
	(C8,2)8			108	45	90	29	
Ar78	(C16,4)6	33	430					
Ar96	(C7)6			[a]	20		23[b]	126
	(C12)6	22	462	[a]	16		20[b]	
	(C16,4)6	22		[a]	6		8[b]	
Ar132	(C16,4)8	33	546					

[a] Liquid crystalline at room temperature. [b] Value at 100 °C. [c] Calculated using eq 2. [d] Temperature at which the crystalline to liquid crystalline phase transition occurs (where appropriate). [e] At room temperature and at temperatures ca. 10 degrees below and above the crystalline solid to liquid crystalline phase transition.

The pulse-radiolysis time-resolved microwave conductivity technique (PR-TRMC), as applied to the study of the conductive properties of discotic materials, has been described fully elsewhere.[3,12,21] Briefly, the bulk solid is contained in a cell consisting of a 1-cm length of Ka-band (26.5−42 GHz) waveguide closed at one end with a metal plate ("short circuit") and flanged at the other end for connection to the microwave detection circuitry. A uniform micromolar concentration of charge carriers is produced in the sample by a nanosecond pulse of ionizing radiation (3 MeV electrons from a Van de Graaff accelerator). Any change in the conductivity of the sample resulting from the formation of mobile charge carriers is monitored (without the need of electrode contacts) as a decrease in the microwave power reflected by the sample cell. The one-dimensional, intracolumnar charge carrier mobility is determined from the end-of-pulse conductivity per unit dose, $\Delta\sigma_{eop}/D$ (Sm^2/J), using the relationship

$$\Sigma\mu_{1D} = 3 \cdot \frac{\Delta\sigma_{eop}}{D} \cdot \frac{E_p}{W_p} \qquad (1)$$

In eq 1, E_p is the average energy deposited in eV per ionization event and W_p is the probability that initially formed ion-pairs survive to the end of the pulse. The value of E_p was taken to be 25 eV, and the values of W_p, which were all within the range 0.36 ± 0.12 for the present compounds, were calculated as described previously.[3,12,21] The factor of 3 in eq 1 takes into account the fact that the organized columnar domains within the bulk samples investigated are randomly orientated and that charge transport is expected to be highly anisotropic and to occur almost exclusively along the axis of the macrocyclic stacks. The mobility sum, $\Sigma\mu = \mu(+) + \mu(-)$, is used in eq 1 since the PR-TRMC technique does not allow the determination of the separate contributions of the positive and negative charge carriers.

Results and Discussion

Optical Absorption. The optical absorption spectra of dilute solutions in chloroform of representative derivatives of all six aromatic cores are shown in Figure 2. In cases where compounds were available for a given core with different peripheral substituents, the nature of the substituent had a negligible influence on the spectrum. In agreement with previous observations on polyaromatic systems,[18] the first absorption band of the present

(19) Piris, J.; Pisula, W.; Tracz, A.; Pakula, T.; Müllen, K.; Warman, J. M. *Liq. Cryst.*, submitted.
(20) van de Craats, A. M.; Warman, J. M. *Adv. Mater.* **2001**, *13*, 130−133.
(21) Schouten, P. G.; Warman, J. M.; de Haas, M. P. *J. Phys. Chem.* **1993**, *97*, 9863−9870.

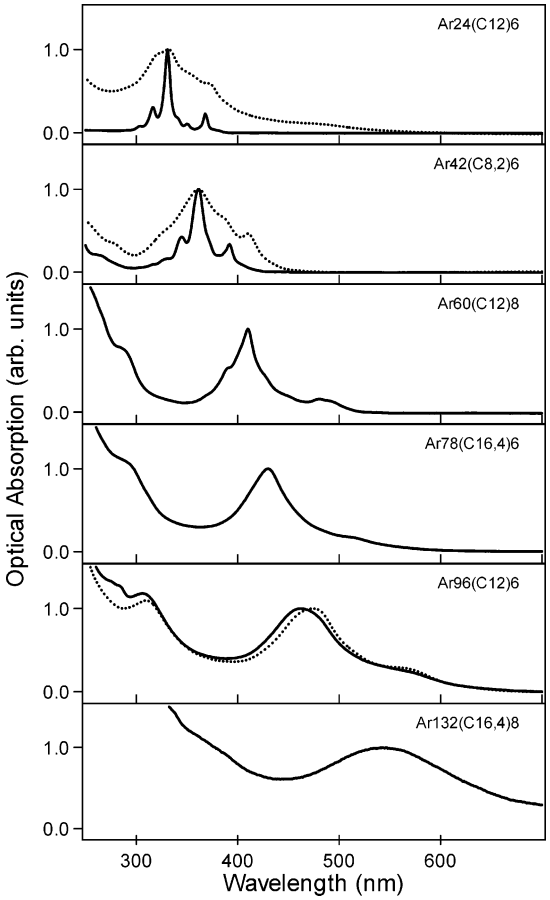

Figure 2. Optical absorption spectra of chloroform solutions (solid lines) and spin-coated films (dotted lines) of selected compounds indicated in the upper right of the figures. All spectra have been normalized to unity at the maximum of the first absorption band.

compounds is seen to undergo a pronounced bathochromic shift with increasing size of the aromatic core, from $\lambda_{max} = 331$ nm for Ar24 to $\lambda_{max} = 546$ nm for Ar132. The values of λ_{max} for the six different cores, which are listed in Table 1, are empirically found to obey a good linear relationship with n given by $\lambda_{max} = 280 + 2n$. A similar direct correlation between λ_{max} and core size has recently been reported.[18] Also apparent in Figure 2 is the increased broadening which accompanies the spectral red-shift.

For the Ar24, 42, and 96 derivatives in Figure 2, it was possible to prepare homogeneous solid films of good optical quality by spin-coating chloroform solutions onto quartz substrates. The absorption spectra of these films are presented in Figure 2 as dotted lines. The spectral features are seen to be considerably broadened in the films of the Ar24 and 42 derivatives which can be attributed to intermolecular interactions in the solid phase. This effect appears to be absent for the Ar96 derivative, possibly because aggregation occurs even in very dilute solutions.[22] For all three compounds, a slight red-shift in the spectral maxima is observed in the solid phase, as found previously for similar compounds.[18] We have no explanation for the appearance of a relatively weak, long-wavelength band at ca. 480 nm for the film of the coronene derivative.

Charge Transport: Room-Temperature Conductivity Transients. Examples of conductivity transients determined at room temperature for representative derivatives of the six different aromatic cores investigated are shown in Figure 3. The measurements were carried out on the freshly prepared materials as received with no prior thermal treatment. As mentioned in the Experimental Section, the extremely low solubility of the Ar78 and Ar132 derivatives made rigorous purification impossible. This undoubtedly explains the fact that for these materials the conductivity saturates within the pulse and rapidly decays to a value close to the signal-to-noise level of the measurements.

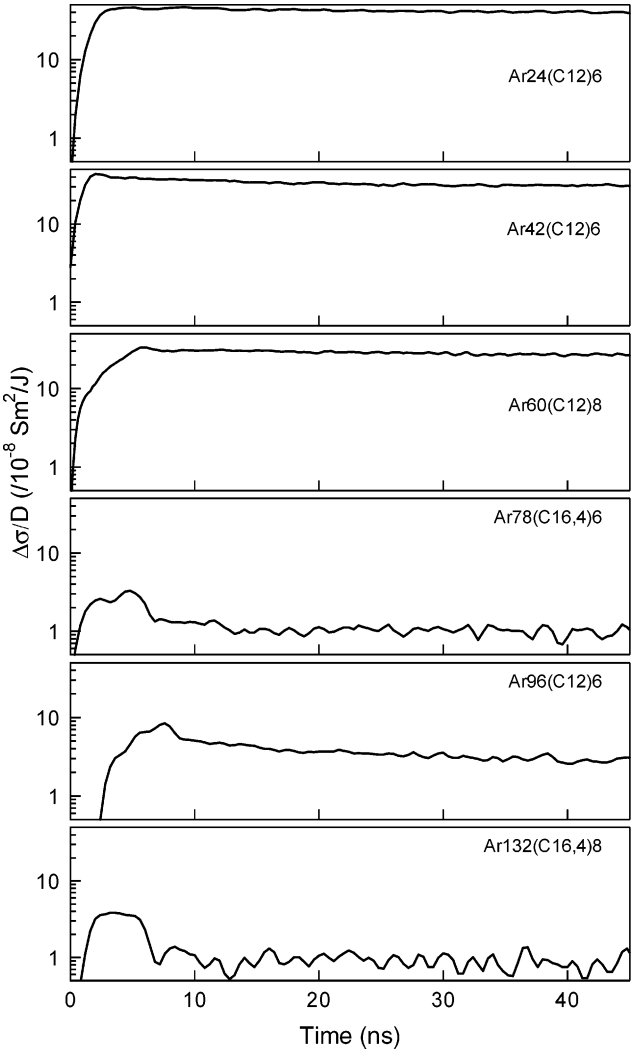

Figure 3. Room-temperature conductivity transients on pulse-radiolysis of bulk samples of the compounds indicated in the upper right of the figure. Note the logarithmic vertical scale.

In this regard, the conductivity measurements are extremely sensitive to only trace impurities which function as trapping centers for mobile charge carriers. For example, a charge carrier with a mobility of 1 cm^2/Vs, characteristic of the present materials, will visit close to 200 different molecular sites within 1 ns during its intracolumnar diffusive motion. Concentrations of less than 1% of trapping sites incorporated within the columnar stacks would therefore be sufficient to result in the short lifetimes observed for the Ar78 and Ar 132 compounds.

As can be seen in Figures 3 and 4, for the Ar24, 42, 60, and 96 derivatives the conductivity grows during the pulse and subsequently decays over time scales which extend from hundreds of nanoseconds to tens of microseconds. Such long lifetimes of the mobile carriers attest to the considerably higher

(22) Tomović, Ž.; Watson, M. D.; Müllen, K. *Angew. Chem., Int. Ed.* **2004**, *43*, 755−758.

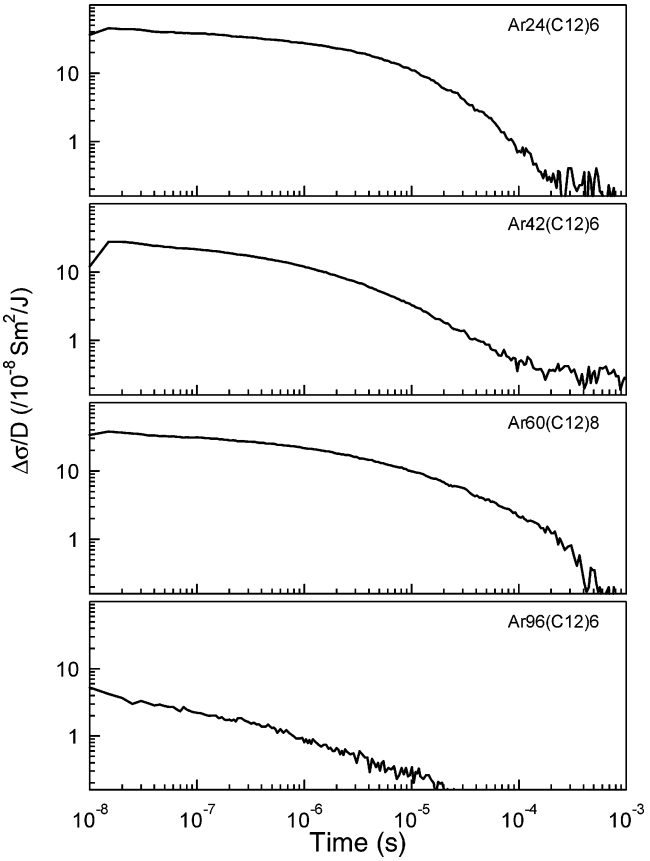

Figure 4. Room-temperature conductivity transients of bulk samples of the compounds indicated in the upper right of the figure from 10 ns to 1 ms. Note the logarithmic vertical *and* horizontal scales.

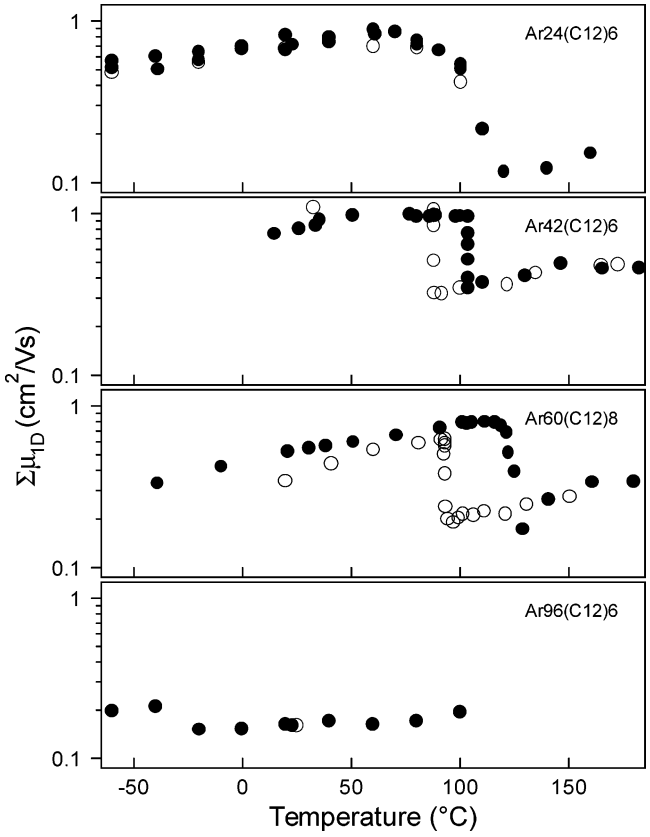

Figure 5. The temperature dependence of the one-dimensional mobility for the first heating (full circles) and cooling (open circles) cycle for the compounds indicated in the upper right of the figure.

purity of these compounds. Since the lifetimes were long compared to the pulse lengths used, accurate values of $\Sigma\mu_{1D}$ could be determined from the end-of-pulse conductivity, and the room-temperature values are listed in Table 1.

For those materials that are crystalline solids at room temperature, the average mobility for a given core shows a tendency to slightly decrease with increasing core size from 0.72 cm^2/Vs for Ar24 to 0.61 cm^2/Vs for Ar42 and to 0.49 cm^2/Vs for Ar60. However, the values for Ar24 and Ar60 lie within the extremes of the values found for the different peripherally substituted Ar42 derivatives. A conservative conclusion from the present, room-temperature data would therefore be that there is in fact no clear-cut trend in mobility with core size for the crystalline phase of the present class of polycyclic aromatic core compounds.

The (PhC12)6 derivative of Ar42 and the three hexakis-*n*-alkyl derivatives of Ar96 are liquid crystalline even at room temperature. The mobilities found for these compounds are all substantially lower than for the compounds which are crystalline solids at room temperature. This follows the general trend of a reduced charge mobility in the mesophase of discotic materials which is attributed to the introduction of dynamic disorder within the columnar stacks on "melting" of the aliphatic side chains. The maximum room-temperature values of $\Sigma\mu_{1D}$ found for the liquid crystalline derivatives of Ar42 and Ar96 are both close to 0.2 cm^2/Vs, indicating again no significant dependence on core size.

The Temperature Dependence of the Mobility. In Figure 5 are shown the mobility values as a function of temperature for the same compounds for which the room-temperature transients are presented in Figure 4. The three compounds that are crystalline solids at room temperature display the same general behavior as found for the majority of discotic materials,[12] that is, a slight, gradual increase of mobility with increasing temperature up to close to the solid-to-mesophase transition temperature, followed by an abrupt decrease as the mesophase is entered. On cooling, the mobility returned to close to the values found for the heating trajectory with a hysteresis of <10, 16, and 30 degrees for Ar24, 42, and 60, respectively.

The mobility values at approximately 10 degrees below and above the transition temperature on heating are listed in Table 1 for all of the compounds which display a room-temperature crystalline phase. In Ar24(C12)6, the range of the mesophase is limited to 20 degrees or less by a transition to a highly fluid (isotropic liquid?) phase which occurs at approximately 115 °C.[23] Only an approximate estimate of $\Sigma\mu_{1D}$ between 0.1 and 0.2 cm^2/Vs for the mesophase of this compound could therefore be derived.

The data for Ar96(C12)6 in Figure 5 display only a gradual increase with temperature with no abrupt change indicative of a phase transition. This behavior is also found for Ar96(C7)6 and Ar96(C16,4)6 and has been previously reported for the (PhC12)6 derivative of Ar42.[11] This is in accordance with the fact that these compounds are already liquid crystalline at room temperature. For comparative purposes, the mobility values for these compounds, given in the penultimate column of Table 1,

(23) Watson, M.; Debije, M. G.; Warman, J. M.; Müllen, K. *J. Am. Chem. Soc.* **2004**, *126*, 766−771.

are for temperatures of approximately 100 °C, that is, close to the $T_c + 10$ temperatures for the room-temperature crystalline materials. As can be seen, the mobilities in the mesophases of all the Ar24, 42, 60, and 96 derivatives lie within the range from ca. 0.1 to 0.4 cm^2/Vs with no general trend with core size apparent. The values found for the present compounds are, however, approximately an order of magnitude larger than the maximum value of 0.025 cm^2/Vs previously found for discotic triphenylene derivatives.[20]

The Core-Size Dependence? On the basis of the maximum values of the mobility found in the mesophase of a variety of discotic materials with different (hetero)aromatic cores, Van de Craats and one of the present authors (JMW) proposed the following empirical relationship between $\Sigma\mu_{1D}$ and the core size.[20]

$$\Sigma\mu_{1D} = 3\exp(-83/n)\ [cm^2/Vs] \qquad (2)$$

The limiting, infinite core, value of 3 cm^2/Vs was taken as the value found for sheet-to-sheet charge transport in graphite.

The values of $\Sigma\mu_{1D}$ calculated using eq 2 for the compounds studied in the present work are given in the last column of Table 1. As can be seen, eq 2 predicts an increase by more than an order of magnitude in going from Ar24 to Ar96 whereas they differ by at most a factor of 2 and the absolute value calculated for the latter is more than a factor of 5 larger than actually measured. Equation 2 is therefore clearly not supported by the present results. We conclude rather that the mobility is in fact relatively insensitive to the size of the aromatic core, at least for core sizes larger than approximately 40.

In recent theoretical work, consideration has been given to the influence on the charge-transfer integral of lateral, longitudinal, and rotational fluctuations within the columnar stacks of discotic materials.[24−26] One of the general conclusions reached was that "an increase in size of the conjugated core does not necessarily ensure better transport properties".[24] The results presented here tend to support this conclusion.

Summary

The optical absorption spectra of dilute solutions of peripherally alkyl-substituted discotic materials with aromatic hydrocarbon cores consisting of 24, 42, 60, 78, 96, and 132 carbon atoms broaden and become increasingly red-shifted with increasing core size. The wavelength maximum of the first absorption band covers the range from 331 to 546 nm and obeys the relationship $\lambda_{max} = 280 + 2n$ with n the number of aromatic carbon atoms. Only a slight red-shift of λ_{max} is found for spin-cast films.

For the derivatives of Ar24, 42, 60, and 96, long-lived mobile charge carriers were observed using the pulse-radiolysis time-resolved microwave conductivity technique. The one-dimensional intracore mobilities, $\Sigma\mu_{1D}$, in the room-temperature crystalline solids of Ar24, 42, and 60 ranged from 0.4 to 1.0 cm^2/Vs. Somewhat lower values were determined in the liquid crystalline mesophases of the Ar24, 42, 60, and 96 derivatives with maximum values, at approximately 100 °C, of 0.15 ± 0.05, 0.38, 0.29, and 0.23 cm^2/Vs, respectively. The recently proposed dependence of $\Sigma\mu_{1D}$ on core size[20] would have predicted an increase by more than an order of magnitude from 0.09 to 1.26 cm^2/Vs over this range of core sizes. Clearly, such an increase is not borne out by the present results.

The large and tailorable spectral coverage of the present class of discotic materials and their, in general, large charge mobilities in both the crystalline and liquid crystalline phases make them potential candidates for applications in molecular optoelectronic devices, in particular, photovoltaic cells for solar energy conversion. Large, monochromatic efficiencies have in fact recently been achieved for photovoltaic cells on the basis of a composite layer of Ar42(PhC12)6 and a perylenediimide derivative.[1] In addition, the capability of forming highly aligned films by self-assembly from solution, which has also recently been demonstrated,[15] has led to the first successful attempt to use aromatic-core discotics in field effect transistors.[2]

Acknowledgment. This work was supported by funds from the EU project DISCEL (G5RD-CT-2000-00321), by the Zentrum für Multifunktionelle Werkstoffe und Miniaturisierte Funktionseinheiten (BMBF 03N 6500), and by the German Science Foundation (Schwerpunktprogramme Organische Feldeffekttransistoren).

JA0395994

(24) Cornil, J.; Lamaur, V.; Calbert, J.-P.; Bredas, J.-L. *Adv. Mater.* **2002**, *14*, 726−729.
(25) Senthilkumar, K.; Grozema, F. C.; Bickelhaupt, F. M.; Siebbeles, L. D. A. *J. Chem. Phys.* **2003**, *119*, 9809−9817.
(26) Lemaur, V.; da Silva Filho, D. A.; Coropceanu, V.; Lehmann, M.; Geerts, Y.; Piris, J.; Debije, M. G.; van de Craats, A. M.; Senthilkumar, K.; Siebbeles, L. D. A.; Warman, J. M.; Brédas, J.-L.; Cornil, J. *J. Am. Chem. Soc.* **2004**, *126*, 3271−3279.
(27) Ito, S.; Wehmeier, M.; Brand, J. D.; Kübel, C.; Epsch, R.; Rabe, J. P.; Müllen, K. *Chem. Eur. J.* **2000**, *6*, 4327−4242.
(28) Herwig, P.; Kayser, C. W.; Müllen, K.; Spiess, H. W. *Adv. Mater.* **1996**, *8*, 510−513.
(29) Fechtenkötter, A.; Saalwächter, K.; Harbison, M. A.; Müllen, K.; Spiess, H. W. *Angew. Chem., Int. Ed.* **1999**, *38*, 3039−3042.
(30) Fischbach, I.; Pakula, T.; Minkin, P.; Fechtenkötter, A.; Müllen, K.; Spiess, H. W.; Saalwächter, K. *J. Phys. Chem. B* **2002**, *106*, 6408−6418.
(31) Fechtenkötter, A.; Tchebotareva, N.; Watson, M.; Müllen, K. *Tetrahedron* **2001**, *57*, 3769−3783.
(32) Iyer, V. S.; Yoshimura, K.; Enkelmann, V.; Epsch, R.; Rabe, J. P.; Müllen, K. *Angew. Chem., Int. Ed.* **1998**, *37*, 2696−2699.
(33) Simpson, C.; Wu, J.; Watson, M. D.; Müllen, K. *J. Mater. Chem.* **2004**, *14*, 494−504.